Published in final edited form as:

Biochem J. 2016 September 15; 473(18): 2783–2798. doi:10.1042/BCJ20160607.

Cdk2 catalytic activity is essential for meiotic cell division *in vivo*

Sangeeta Chauhan[1], **M. Kasim Diril**[1,*], **Joanna H.S. Lee**[1], **Xavier Bisteau**[1], **Vanessa Manoharan**[1], **Deepak Adhikari**[2,†], **Chandrahas Koumar Ratnacaram**[1], **Baptiste Janela**[3], **Juliane Noffke**[1], **Florent Ginhoux**[3], **Vincenzo Coppola**[4,‡], **Kui Liu**[2], **Lino Tessarollo**[4], **Philipp Kaldis**[1,5]

[1]A*STAR (Agency for Science, Technology and Research), Institute of Molecular and Cell Biology (IMCB), 61 Biopolis Drive, Proteos#3-09, Singapore 138673

[2]Department of Chemistry and Molecular Biology, University of Gothenburg, SE-405 30 Gothenburg, Sweden

[3]A*STAR (Agency for Science, Technology and Research), Singapore Immunology Network (SIgN), 8A Biomedical Grove, Immunos, Singapore 138648

[4]National Cancer Institute, Mouse Cancer Genetics Program, NCI-Frederick, Bldg. 560, 1050 Boyles Street, Frederick, MA 21702-1201, USA

[5]Department of Biochemistry, National University of Singapore (NUS), Singapore 117597

Abstract

Cyclin-dependent kinases (Cdks) control the eukaryotic cell cycle by phosphorylating serine and threonine residues in key regulatory proteins, but some Cdk family members may exert kinase-independent functions that cannot easily be assessed using gene knockout approaches. While Cdk2-deficient mice display near-normal mitotic cell proliferation due to the compensatory activities of Cdk1 and Cdk4, they are unable to undergo meiotic generation of gametes and are consequently sterile. To investigate whether Cdk2 regulates meiosis via protein phosphorylation or by alternative kinase-independent mechanisms, we generated two different knockin mouse strains in which Cdk2 point mutations ablated enzyme activity without altering protein expression levels. Mice homozygous for the mutations $Cdk2^{D145N/D145N}$ or $Cdk2^{T160A/T160A}$ expressed only 'kinase-dead' variants of Cdk2 under the control of the endogenous promoter, and despite exhibiting normal expression of cell cycle regulatory proteins and complexes, both mutations rendered mice sterile. Mouse cells that expressed only 'kinase-dead' variants of Cdk2 displayed

Correspondence: Philipp Kaldis (kaldis@imcb.a-star.edu.sg).

*Present address: Izmir Biomedicine and Genome Institute, Dokuz Eylul University, 35340 Izmir, Turkey.

†Present address: School of Biomedical Sciences, Nursing and Health Sciences, Monash University, Clayton, VIC 3800, Australia.

‡Present address: Department of Molecular Virology, Immunology and Medical Genetics, The Ohio State University, 988 Biomedical Research Tower, 460 West 12th Avenue, Columbus, OH 43210, USA.

Author Contribution

S.C., M.K.D., J.H.S.L., X.B., V.M., D.A., C.K.R., B.J., J.N., and V.C. performed experiments; S.C., M.K.D., J.H.S.L., X.B., V.M., D.A., C.K.R., B.J., J.N., V.C., F.G., K.L., L.T., and P.K. contributed to analysis and interpretation of data; F.G., K.L., L.T., and P.K. supervised the study. P.K. wrote the manuscript with feedback from all authors.

Competing Interests

The authors declare that there are no competing interests associated with the manuscript.

normal mitotic cell cycle progression and proliferation both *in vitro* and *in vivo*, indicating that loss of Cdk2 kinase activity exerted little effect on this mode of cell division. In contrast, the reproductive organs of Cdk2 mutant mice exhibited abnormal morphology and impaired function associated with defective meiotic cell division and inability to produce gametes. Cdk2 mutant animals were therefore comparable to gene knockout mice, which completely lack the Cdk2 protein. Together, our data indicate that the essential meiotic functions of Cdk2 depend on its kinase activity, without which the generation of haploid cells is disrupted, resulting in sterility of otherwise healthy animals.

Introduction

Cyclin-dependent kinases (Cdks) are critical regulators of cell cycle progression in eukaryotic cells via the phosphorylation of key substrates involved in DNA replication and mitosis [1]. Cdk2 regulates the G1/S-phase transition and DNA replication, but mouse knockouts for Cdk2 remain viable most likely due to the compensatory activities of Cdk1 and Cdk4 [2–9]. While Cdk2 appears to be nonessential for mitotic cell cycle progression, this protein is crucial for meiotic cell division since Cdk2 knockout (Cdk2KO) mice are sterile due to defective gametogenesis [5,9]. Given that Cdk2 is a protein kinase, it is thought to exert its function via protein phosphorylation. However, kinase-independent functions have recently been reported for other key cell cycle regulators, including cyclin E [10,11], cyclin D [12,13], and Cdk6 [14], but it is currently unknown whether the kinase activity of Cdk2 is required for meiotic cell division *in vivo*.

To assess the requirement for Cdk2 kinase activity in meiotic cell division, we aimed to generate a mouse model in which enzymatically inactive Cdk2 was expressed at normal physiological levels *in vivo*. Unlike Cdk2 gene deletion, this approach allows the Cdk2 protein to express normally and to form complexes with cyclins, avoiding an excess of free cyclin proteins and preventing compensatory activation of other Cdks (as previously observed in Cdk2KO somatic cells [4,8]). Mutation of specific residues affects the activity of Cdk2 [15–19] and we sought to use a minimally disruptive approach of generating two different mouse strains that each exhibited a single point mutation in an individual residue of the Cdk2 protein. The first point mutation targeted the essential residue Asp145, which is present in all Cdk proteins and co-ordinates Mg^{2+} ions to orientate ATP molecules for catalysis [20,21]. Mutation of Asp145 (aspartic acid to asparagine mutation, D145N) renders the Cdk2 protein inactive and can induce cell cycle arrest when overexpressed in human cell lines [22–24]. The second point mutation targeted residue Thr160 (threonine to alanine mutation, T160A), which is phosphorylated during Cdk2 activation by the Cdk-activating kinase [17,20,21,25–30]. We used knockin (KI) techniques to generate mice that expressed these ‘kinase-inactive’ forms of Cdk2 at levels comparable with the wild-type (WT) protein and then assessed whether the constituent cells were still able to divide normally *in vitro* and *in vivo*.

Materials and methods

Generation of Cdk2^{D145N} and Cdk2^{T160A} KI mice

Mouse genomic DNA harboring the Cdk2 locus was subcloned from pBeloBACII 192B20 (ResGEN, #96021) into the pBlight-TK vector as described previously [5]. A neomycin-selection cassette flanked by FRT sites was introduced to the 3′ end of exon 4 using a recombineering technique [31]. D145N and T160A point mutations were introduced to exon 4 using mutagenic primer pairs PKO956/957 and PKO959/960. The resulting targeting vectors PKB1021 (Cdk2^{D145N}) and PKB1022 (Cdk2^{T160A}) were linearized by NotI digestion and then electroporated into embryonic stem (ES) cells (Supplementary Figure S1A). Following positive and negative selection with geneticin and ganciclovir, respectively, genomic DNA from the surviving ES cell colonies was used to screen for homologous recombination by Southern hybridization (PstI digest for 5′ probe [PKO116–117] and BspHI digest for 3′ probe [PKO1336–1337]). Correctly targeted ES cell clones (D145N: 7510, 7519, 7520, 7525; T160A: 8015, 8016, 8044, 8045) were identified and used for the generation of the Cdk2 KI mouse strains. To generate the final Cdk2 KI alleles (Supplementary Figure S1A, row IV), the neomycin cassette was removed by crossing the mice with β-actin–Flpe transgenic mice [32] [strain name: B6.Cg-Tg(ACTFLPe) 9205 Dym/J; stock no. 005703; The Jackson Laboratory]. The presence of the point mutations in the KI mice was verified by sequencing of DNA from tail snips (Supplementary Figure S1C). Heterozygote mice were crossbred to generate Cdk2$^{D145N/D145N}$ and Cdk2$^{T160A/T160A}$ homozygous mice. For mouse genotyping, we used a polymerase chain reaction (PCR) protocol that yields a longer product for either of the KI alleles due to the presence of an FRT site (Supplementary Figures S1A, row IV, and S1D). Mice were routinely genotyped by isolating genomic tail DNA using HotSHOT lysis [33]. A total of 1 μl genomic DNA was used as the template in a 20 μl PCR reaction, using 0.5 units of MangoTaq polymerase (Fermentas) using the following protocol: 35 PCR cycles with 30 s denaturation at 94°C, 30 s annealing at 60°C, and 30 s extension at 72°C. Amplification of the WT or mutant Cdk2 alleles then resulted in bands of either 224 bp (Cdk2^{WT}) or 256 bp (Cdk2^{D145N} or Cdk2^{T160A}) (Table 1).

Mice were housed under standard conditions (12 h light/dark cycle) with food and water available *ad libitum*. Mice were fed a standard chow diet containing 6% crude fat and were treated humanely in compliance with the Institutional Animal Care and Use Committee (IACUC) guidelines.

Isolation and culture of primary mouse embryonic fibroblasts

Primary mouse embryonic fibroblasts (MEFs) were isolated from E13.5 mouse embryos as described previously [5]. Briefly, the head and the visceral organs were removed, the embryonic tissue was chopped into fine pieces using a razor blade, trypsinized for 20 min at 37°C, and then subjected to vigorous pipetting to dissociate cell clumps. Cells were plated into 10 cm culture dishes (passage 0) and grown in DMEM (Invitrogen 12701–017), supplemented with 10% fetal calf serum (Invitrogen 26140) and 1% penicillin/streptomycin (Invitrogen 15140–122). Primary MEFs were cultured in a humidified incubator with 5% CO_2 and 3% O_2.

Proliferation assay, BrdU labeling, and FACS analysis

All cell-based experiments were performed using primary MEFs isolated from three different embryos of matching genotype from the same litter (genotype confirmed by sequencing). Experiments were conducted using passage 2 cells.

For Alamar Blue proliferation assays, 1500 cells were plated into 96-well plates in triplicate. After 24 h, the cells were incubated with 150 μl of assay medium [1:9 ratio of Alamar Blue (AbD Serotec, BUF012B) to growth medium] for 4 h, and metabolic activity was quantified by measuring fluorescence emission at 590 nm.

For BrdU labeling and FACS analysis, MEFs were grown to confluence in 15 cm dishes and serum-starved for 72 h in growth medium containing 0.2% serum. To induce synchronized re-entry into cell cycle, the cells were trypsinized and re-plated into 10 cm dishes with complete growth medium. Cells were pulse-labeled with 100 μM BrdU (BD Pharmingen, #550891) for 1 h before harvesting. At each time point, the cells were trypsinized and fixed in ice cold 70% ethanol. BrdU staining was conducted as previously described in Diril et al. [34]. Cell cycle analysis was performed using an FACSCalibur flow cytometer (BD Biosciences) and FlowJo software.

Histology

For hematoxylin and eosin (H&E) staining, testes and ovaries were isolated at the indicated time points and fixed either in Bouin's fixative (Sigma-Aldrich, HT10132) or 10% neutral buffered formalin (Sigma-Aldrich, HT501128), then transferred into 70% ethanol, embedded in paraffin, and cut into 6 μm sagittal sections with a microtome. To evaluate proliferation in ovary, histological sections were stained using Ki-67 antibodies (Leica Microsystems, NCL-Ki67p). Images were captured using either an Olympus BX61 or Zeiss Imager Z1 microscope.

Western blots, immunoprecipitations, and kinase assays

Cells and embryonic tissues were lysed in EBN buffer [80 mM β-glycerophosphate pH 7.3, 20 mM EGTA, 15 mM $MgCl_2$, 150 mM NaCl, 0.5% NP-40, 1 mM DTT, protease inhibitors (20 μg/ml each of leupeptin (EI8), chymostatin (EI6), and pepstatin (EI10) from Chemicon)] for 20 min under constant shaking at 1200 rpm. Lysates were centrifuged at 18 000 × *g*, 4°C for 30 min, and supernatants were snap-frozen in liquid nitrogen for storage at −80°C until analysis. A total of 10–15 μg of protein extracts were separated on 10 or 12.5% polyacrylamide gels, transferred via a semidry system onto polyvinylidene difluoride membranes (Millipore, IPVH0010), and then blocked in Tris-buffered saline with 0.1% Tween 20 and 5% nonfat dry milk (Bio-Rad, 1706404). Blots were probed with the indicated primary antibodies overnight at 4°C, followed by secondary goat antimouse (Pierce, 0031432) or antirabbit antibodies (Pierce, 0031462) conjugated with horseradish peroxidase, and were developed using enhanced chemiluminescence (PerkinElmer, NEL105001EA). All antibodies used for immunoblotting were obtained from commercial suppliers: mouse anti-Cdk1 (Santa Cruz, sc-54), mouse anti-Cdk2 (Santa Cruz, sc-6248), mouse anti-Cdk4 (Cell Signaling, #2906), rabbit anti-cyclin A2 (Santa Cruz, sc-596), mouse anti-cyclin A2 (Biosource, AHF0022), mouse anti-cyclin B1 (Cell Signaling, #4135), mouse anti-cyclin D1

(Cell Signaling, #2926), rabbit anti-cyclin E1 (eBioscience, 146714), mouse anti-p21 (Santa Cruz, sc-6246), mouse anti-p27 (BD Transduction, 610242), mouse anti-Cdc6 (Santa Cruz, sc-9964), rabbit anti-MCM2 (Cell Signaling, #3619), rabbit anti-Stat1 (Cell Signaling, #9172), rabbit anti-Stat3 (Cell Signaling, #9132), mouse anti-α-tubulin (Sigma, F2168), mouse anti-γ-tubulin (Sigma, T6557), mouse anti-Hsp90 (BD Transduction, 610419), and goat anti-actin (Santa Cruz, sc-1616).

Affinity purification/immunoprecipitations (IPs) and kinase assays were performed as described previously [5] with minor modifications. Briefly, 50–250 μg of protein extract was incubated with proteins/antibodies that were either covalently conjugated with agarose beads (for Cdk2 [5], cyclin B1 [Santa Cruz, sc-7393], cyclin A2 [Santa Cruz, sc-751], and suc1 [Upstate, 14–132]), or unconjugated (for Cdk1 [Santa Cruz, sc-954]). Unconjugated antibodies together with bound proteins were isolated the following day by incubation for 1 h with protein A agarose beads (Roche, 11719408001). After four washes in EBN buffer and one wash in EB buffer (EBN without NP-40), the precipitated proteins were either resolved by SDS–PAGE for Western blot (WB) analysis or used in kinase assays to determine the levels of enzyme activity against the substrate histone H1 (Roche, 11004875001). Kinase assays were performed by incubating the immunoprecipitated, bead-bound proteins in EB buffer supplemented with 10 mM DTT, 15 μM ATP, 5 μCi [Υ-P^{32}]ATP (PerkinElmer, NEG502A), and 1.5 μg histone H1 for 30 min at room temperature. The assay mixture was then inactivated in SDS–PAGE sample buffer and subjected to electrophoresis on polyacrylamide gel, then fixed and stained in Bismarck Brown/Coomassie blue prior to quantification of incorporated radioactivity using a PhosphoImager (Fujifilm, FLA-7000).

RNA analysis

Total RNA was extracted using the Qiagen RNeasy Mini Kit according to the manufacturer's protocol. For each qPCR reaction, first-strand cDNA was synthesized from 0.2 μg of total RNA using the SuperScript III reverse transcriptase (Invitrogen, 18080–051) according to the manufacturer's protocol. qPCR primers were designed for each target gene as presented in the table below. PCR amplification was carried out using the Maxima SYBR Green qPCR Master Mix (Fermentas, K0252) and reactions were monitored continuously in a Rotor-Gene thermal cycler (Corbett Research) with the following program: 95°C for 10 min, followed by 40 cycles of 95°C for 15 s, 55°C for 30 s, and 72°C for 30 s. All data were normalized to the expression levels of housekeeping genes β-actin or Hsp90 (Table 2).

Thymus analysis

Thymus tissue was incubated for 1 h at 37°C in collagenase digestion mixture (0.1 mg/ml collagenase type 4 in calcium-replete HBSS containing 10% FCS and 200 U/ml DNase). After homogenization and filtration, the resultant cells were stained and analyzed using an LSRII flow cytometer together with FlowJo software (Tree Star) as has been described [35,36]. Biotin-conjugated anti-CD90.2 (53–2.2), eFluor605NC-conjugated anti-CD19 (1D3), APC-conjugated anti-CD4 (GK1.5), eFluor450-conjugated anti-CD8 (53–6.7), and PE-Cy7-conjugated anti-CD3 (145–2C11) were purchased from eBioscience, whereas APC-Cy7-conjugated anti-CD45 (30-F11) was obtained from BD Pharmingen. Biotin-conjugated antibodies were detected using streptavidin conjugated with PE-TexasRed (Invitrogen).

Mann–Whitney *t*-tests (with a 95% confidence interval) were performed using Prism 6.0 (GraphPad Software, La Jolla, USA). All *P*-values are two-tailed (*$P < 0.05$, **$P < 0.01$, and ***$P < 0.001$).

Testis chromosome spreads and immunofluorescence analysis

Meiotic chromosome spreads were prepared as previously described [37,38] with small modifications. Briefly, testes were excised from male mice killed at postnatal day 23 or at 1 month old, and placed in PBS. The tunica albuginea was removed and the seminiferous tubules were gently teased apart with blunt forceps. The seminiferous tubules were placed in hypotonic extraction buffer (30 mM Tris pH 8.2, 50 mM sucrose, 17 mM trisodium citrate dihydrate, 5 mmM EDTA) and incubated for an hour with gentle rotation at room temperature. Small portions of the seminiferous tubules were placed in 100 µl of 100 mM sucrose droplets, pH 8.2 and pipetted repeatedly (~50 times) using a cut 200-µl tip until the solution turned turbid. Tubular remnants were removed from the suspension. Polylysine-coated slide was dipped in freshly prepared fixative (1% PFA, 30 mM sodium tetraborate pH 9.2 and 0.15% Triton X-100) and the seminiferous tubule suspension was placed at the edge of the slide and allowed to drip along the length of the slide. The prepared slides were placed in a humidified chamber at 4°C for 6–12 h and stored at −20°C until further use.

For immunofluorescence analysis, slides with chromosome spreads were washed three times with PBS, followed by incubation for 1 h with blocking buffer (PBS with 0.1% Tween-20 and 10% donkey serum) in a humidified chamber at room temperature. Chromosome spreads were incubated with primary antibodies [SYCP3 (M-14) — Santa Cruz Biotechnology, #20845; Cdk2 (D-12) — Santa Cruz Biotechnology, #SC-6248; SUN1 — Gift from Brian Burke; Phospho-H2AX (Ser139) — Upstate, #07–164; SYCP1 — Abcam, #AB15090] diluted in blocking buffer and incubated overnight at 4°C. Slides were washed three times in PBST (PBS with 0.1% Tween-20) and incubated for an hour at room temperature with appropriate Alexa (488/555)-conjugated secondary antibodies (Molecular Probes) diluted in blocking buffer. Slides were washed three times in PBST, followed by 100 ng/ml DAPI counterstaining for 1 min before mounting on the cover slips. Images were taken using a Zeiss AxioImager Z1 epifluorescence microscope with Zeiss AxioCam MRc5 at 63× objective (Zeiss Plan-APOCHROMAT, 63×/1.4 Oil DIC, ∞/0.17).

Results

Physiological expression of ‘kinase-dead’ Cdk2 confers mouse sterility

To investigate the role of Cdk2 catalytic activity *in vivo*, we assessed the effects of two different point mutations that disrupt the enzyme activity without impacting its cyclin binding capacity [16]: the Asp145 mutation D145N, which prevents coordination of ATP and blocks phospho-transfer within the catalytic core of the enzyme [20,24], and the Thr160 mutation T160A, which disrupts the phosphorylation event required for Cdk2 activation [15,16,19]. We constructed two separate targeting vectors that enabled us to modify Cdk2 exon 4 by introducing either the D145N or T160A mutation, thereby generating $Cdk2^{D145N}$ and $Cdk2^{T160A}$ KI mutant mouse strains (Supplementary Figure S1A). Homologous recombination was confirmed by Southern blot analyses (Supplementary Figure S1B), and

the presence of the KI mutations in exon 4 was verified by sequencing and genotyping PCR (Supplementary Figure S1C,D). When we intercrossed heterozygous mutant mice, the proportion of homozygous offspring born was below the expected Mendelian distribution (Table 3), especially for D145N (14% instead of the expected 25%). As observed in Cdk2KO mice [5], Cdk2 KI mutants were slightly smaller than WT littermates. Anatomical and histological examination of mutant mice revealed that there were no apparent malformations, except that there was noticeable difference in the size of testes and ovaries. Mating between homozygous KI males and females did not result in pregnancies. Similar observations were made when homozygous KI mutants were kept for breeding with WT mice, indicating that both male and female mice with homozygous Cdk2 knocking mutations are viable but sterile, and therefore closely resembled the phenotype of Cdk2KO mice [5,9]. These data suggest that ablation of Cdk2 kinase activity alone is sufficient to replicate the fertility defects conferred by complete protein deletion.

Cdk2 KI MEFs proliferate efficiently

The KI mutants displayed a reduction in the proportion of homozygous offspring born and of the size of testis and ovaries, especially in the case of D145N mutant. Nevertheless, mechanistic studies directly in these tissues are difficult to perform since genetic *in vivo* experiments take a long time and there is a lack of *in vitro* tools. Previous *in vitro* studies reported that human cell lines overexpressing $Cdk2^{D145N}$ failed to enter S-phase and remained arrested in G1 [22,24], whereas overexpression of the $Cdk2^{T160A}$ mutant had no apparent effect on cell proliferation. Given the fact that there is a wealth of information on Cdk2KO MEFs [4,5,8,9,39–44], we next sought to determine whether KI mutations alter the cell cycle progression and the expression of its regulators in MEFs. We therefore investigated whether the expression of ‘kinase-dead’ Cdk2 protein could also led to defects in cell cycle progression and proliferation. However, we observed that overall rates of proliferation of primary MEFs from $Cdk2^{D145N}$ and $Cdk2^{T160A}$ mice were comparable to WT cells (Figure 1A). Similarly, the expression levels of the majority of key cell cycle regulatory proteins checked were comparable across the different genotypes (Supplementary Figure S2A). The only exceptions were the marginally increased levels of cyclin E1 detected in $Cdk2^{D145N}$ MEFs, and the slight elevation of p21 protein expression observed in both KI mutants (Supplementary Figure S2A). When we assessed mRNA expression profiles in the mutants using quantitative real-time PCR, we detected increased levels of cyclin E1 mRNA in both point mutants, as well as a slight up-regulation of cyclin A2 mRNA in $Cdk2^{D145N}$ MEFs (Supplementary Figure S2B). Expression levels of $Cdk2^{T160A}$ mRNA were slightly higher than those detected for the WT, whereas levels of $Cdk2^{D145N}$ mRNA were lower compared with those detected for WT Cdk2. The two-fold increase in Cdk1 mRNA expression in $Cdk2^{D145N}$ mutants (Supplementary Figure S2B) is suggestive of a potential compensatory response to the loss of Cdk2 kinase function.

We next investigated the ability of the mutant Cdk2 protein to form complexes with different cyclins and observed that immunoprecipitates of Cdk1, Cdk2, cyclin A2, and cyclin E1 formed with comparable efficiency in the mutant and WT cells (Figure 1B). Although Cdk2/cyclin A2 complexes appeared to assemble somewhat less efficiently in $Cdk2^{T160A}$ MEFs, the overall pattern of Cdk/cyclin complex formation was not greatly affected by the Cdk2 KI

mutations. We therefore proceeded to assess whether loss of Cdk2 enzyme activity could alter the kinase activities of other Cdks and cyclin proteins. Consistent with earlier studies using purified proteins [16,18,22], our analyses of immunoprecipitates of Cdk2 or cyclin E1 from the KI mutants were unable to detect any kinase activity for the substrate histone H1 (Figure 1C). While we did detect a minimal increase in Cdk1-associated kinase activity in the $Cdk2^{D145N}$ cell extracts, the enzymatic activities of all other tested immunoprecipitates were comparable to WT (Figure 1C), indicating that loss of Cdk2 catalytic activity does not substantially alter the function of other Cdk family members or cyclin proteins. Since both point mutations were sufficient to induce sterility in the mutant mice without affecting significantly the expression of key cell cycle regulatory proteins or complexes, the mouse sterility was likely caused due to the loss of Cdk2 kinase activity and not due to the lack of Cdk2 protein.

$Cdk2^{D145N}$ is not a dominant-negative mutation

The majority of the experiments presented in our study were performed using homozygous $Cdk2^{D145N}$ mice or MEF derived from them, which express mutant Cdk2 protein at levels equivalent to the WT Cdk2 locus. While the homozygous mutants were very similar to Cdk2KO mice with respect to the phenotypes described here, heterozygous $Cdk2^{+/D145N}$ mice and their derivative cells were phenotypically comparable to WT. Given that $Cdk2^{D145N}$ was originally described as a dominant-negative mutation [24], but did not appear to adversely affect cell functions in our assays, we next assessed the molecular profile of heterozygous $Cdk2^{+/D145N}$ MEFs. All cell cycle regulatory proteins and complexes tested were expressed/formed at comparable levels between WT, $Cdk2^{+/145N}$, and $Cdk2^{D145N/D145N}$ MEFs (Supplementary Figure S2C). The only exception was cyclin E1, which displayed a step-wise increase in expression and protein binding to Cdk1 and Cdk2 between WT and heterozygous cells, and between heterozygous and homozygous cells (Supplementary Figure S2C,D).

We next determined the kinase activity in $Cdk2^{+/D145N}$ MEFs in comparison with WT and homozygous $Cdk2^{D145N/D145N}$ cells (Figure 1D). Cdk2-associated kinase activity was substantially decreased in $Cdk2^{+/D145N}$ MEFs compared with their WT counterparts, whereas kinase activity was entirely absent in $Cdk2^{D145N/D145N}$ MEFs (Figure 1C,D). The cyclin A2-associated kinase activity followed a similar pattern, although there was still a low level of kinase activity detected in the homozygous mutant MEFs. Cdk1 activity displayed an inverse pattern, with an intermediate amount being detectable in $Cdk2^{+/D145N}$ MEFs, and a substantial increase evident in $Cdk2^{D145N/D145N}$ MEFs (Figure 1D). These results indicate that unlike $Cdk2^{D145N}$ overexpression, which likely leaves no free cyclins to partner with WT Cdk2 or Cdk1, our strategy of expressing $Cdk2^{D145N}$ under the control of its own promoter does not exert dominant-negative effects in MEFs.

$Cdk2^{D145N}$ and $Cdk2^{T160A}$ MEFs exhibit normal cell cycle progression and transformation

Having established that sterility in mice that lack Cdk2 kinase function could not be attributed to effects on cyclin complex formation or enzymatic activity of related proteins, we next investigated whether the expression of these mutants have an impact on normal cell cycle progression. We therefore performed cell cycle progression experiments by arresting

early passage MEFs in a quiescent G0/G1 state (via contact inhibition and serum starvation for 72 h) followed re-seeding low-density culture in complete medium to trigger synchronized re-entry into the cell cycle and by pulse labeling with BrdU. Analysis by flow cytometry revealed that WT MEFs started to enter S-phase at approximately 16 h, with a peak BrdU incorporation rate at 20 h, whereas both KI mutants exhibited a short delay before entering S-phase (Figure 2A,B). This delay prior to S-phase entry resembled previous observations in Cdk2KO MEFs [5,9], suggesting that loss of Cdk2 kinase activity confers a mild delay in cell cycle progression, but does not impair the successful completion of that cell cycle.

We next assayed the kinase activities of various Cdk/cyclin complexes isolated at different time points after cell cycle entry. In WT MEFs, Cdk/cyclin kinase activity was detectable 18–20 h after cell cycle release and peaked approximately 24–28 h (Figure 2C). As expected, Cdk2-associated kinase activity was absent in $Cdk2^{D145N}$ and $Cdk2^{T160A}$ MEFs for the entire duration of the time course. WT and $Cdk2^{T160A}$ mutant MEFs exhibited comparable levels of kinase activity associated with complexes of Cdk1/cyclin A2 and B1, whereas enzymatic efficacy of cyclin A2 was markedly reduced in $Cdk2^{D145N}$ cells (Figure 2C). Taken together, these data indicated that the $Cdk2^{D145N}$ and $Cdk2^{T160A}$ mutations exert differential effects on the kinase activity of associated proteins, but result in the same sterility phenotype.

Cdk2 activity has previously been identified as being crucial for the centrosome duplication cycle [45,46]; therefore, we next assessed whether this process could proceed normally in the absence of Cdk2 kinase function. To study this, we used small hairpin ribonucleic acid (shRNA) silencing of p53 to induce centrosome amplification in homozygous $Cdk2^{D145N}$ and WT MEFs [46,47], and observed that these cells displayed comparable levels of centrosome amplification subjected to the same treatment (Supplementary Figure S3). These data suggested that the requirement for Cdk2 activity in centrosome duplication can be substituted by Cdk1, as has been shown in Cdk2KO MEFs previously [39]. Similar data were obtained when using the alternative approach of inducing centrosome amplification by treating cells with 2 mM hydroxyurea (data not shown) [48]. These data confirm that this key function of G1/S phase transition is not impeded by the loss of Cdk2 kinase activity.

Since immortalization or transformation of primary cells is typically associated with increased Cdk activity, we next tested whether $Cdk2^{D145N}$ MEFs could be successfully transformed using retroviral vectors encoding (i) c-myc/activated H-Ras, (ii) shRNAs against p53, or (iii) activated H-Ras/$p53^{DN}$. Using colony formation assays as our readout, we observed that $Cdk2^{D145N}$ MEFs could be readily transformed or immortalized *in vitro*, and generated slightly a higher number of colonies than WT MEFs (Figure 3). Taken together, these data indicated that transformation, immortalization, and centrosome duplication in MEFs are not impaired by the loss of Cdk2 kinase function, indicating that Cdk1 is fully compensating in these processes.

Cdk2 kinase function is required for cell division in testis but not in thymus

We next proceeded to investigate whether the sterility arising from the expression of $Cdk2^{D145N}$ or $Cdk2^{T160A}$ was due to the loss of kinase function in specific tissues rather

than global effects of the mutation. We observed that WT Cdk2 displayed the highest activity in testis, followed by thymus and spleen, whereas $Cdk2^{D145N}$ did not exhibit kinase activity in any of these tissues (Supplementary Figure S4A, lanes 2 and 4). The kinase activity associated with cyclin B1 or suc1 (reflecting the enzyme function of both Cdk1 and Cdk2) was slightly elevated in spleen and thymus from $Cdk2^{D145N}$ animals, suggesting that Cdk1 may partially compensate for the loss of Cdk2 kinase activity in these tissues. Interestingly, Cdk1/cyclin B1-associated kinase activity was substantially reduced in the testis of $Cdk2^{D145N}$ mice (Supplementary Figure S4A, lane 6). This finding suggested a lack of proliferating cells and inability of Cdk1 to compensate for the loss of Cdk2 kinase function in this tissue, which is a comparable phenotype to what was previously identified in the testes of Cdk2KO mice [5,9].

Although the expression and complex formation between Cdks and cyclins in spleen and thymus of $Cdk2^{T160A}$ animals was comparable to WT (Supplementary Figure S4B–D), we did observe increased binding of p27 to Cdk1 in the mutant thymus (Supplementary Figure S4D, lane 2). In addition, cyclin E1 protein expression was found to be increased in the thymus of $Cdk2^{D145N}$ mice compared with other tissues (Supplementary Figure S4B, lane 4, and Supplementary Figure S5A). To investigate the impact of increased cyclin E1 levels in thymus, we next analyzed whether loss of Cdk2 kinase activity has an impact on thymic selection in the KI animals. We observed that relative to WT, the kinase-dead mutant $Cdk2^{D145N}$ increased the absolute number of $CD4^{-}CD8^{-}$ double-negative T cells in the thymus, but did not significantly alter numbers of $CD4^{+}$, $CD4^{low}CD8^{+}$, $CD8^{+}$, $CD4^{+}CD8^{low}$, or $CD4^{+}CD8^{+}$ double-positive populations (Supplementary Figure S5B,C). Our data indicate that while expression of $Cdk2^{D145N}$ increased the total number of early precursor cells in the thymus, this mutant did not alter the balance of major T-cell populations generated by positive and negative selection.

Reproductive organs display abnormal morphology and function in Cdk2 KI mice

Since kinase-inactive Cdk2 did not exert major effects on the cellular phenotype in MEFs and the compensatory activity of other Cdk family members may play a minor role, we next investigated how the loss of Cdk2 kinase function affected the development of gonads *in vivo*. To this end, we prepared histological sections from the ovaries of female mice and assessed cell proliferative activity using H&E staining together with antibody labeling for the proliferation marker Ki67 (Figure 4). At 5 weeks of age, the ovaries of $Cdk2^{D145N}$ mice were substantially smaller, exhibited fewer follicles, and displayed reduced Ki67 staining compared with age-matched ovaries from WT mice (Figure 4A–C). By 8 weeks of age, $Cdk2^{D145N}$ mice were entirely devoid of ovarian follicles and only trace numbers of Ki67-positive cells were detectable (Figure 4E). A milder phenotype was observed in the ovaries of $Cdk2^{T160A}$ mice (Figure 4F). However, with increasing age, these animals also exhibited fewer follicles and displayed a similar reduction in Ki67-positive cells relative to WT mice (Figure 4I). The phenotype observed in ovary tissues from $Cdk2^{D145N}$ mice, and in aged $Cdk2^{T160A}$ mice, was almost identical with that observed in ovaries from Cdk2KO mice [5,9,49]. Indeed, $Cdk2^{T160A}$ females failed to reproduce even at younger ages when ovaries contained several normal-looking follicles and eggs (Figure 4C), suggesting the presence of a cellular defect that was not revealed by the staining methods used here. There was a

similar age-dependent deterioration in the morphology of reproductive organs in Cdk2 KI males, with $Cdk2^{D145N}$ mice displaying severe testicular dystrophy (Supplementary Figure S6) comparable to that observed in Cdk2KO animals [5,9]. While testis morphology in 3-week-old (Day 21) $Cdk2^{T160A}$ mice appeared largely normal, this mutation was again associated with age-related decline in tissue morphology.

To compare the phenotype in testes of the KI to Cdk2KO animals, we further analyzed the gametogenesis block by isolating the testes of 23-day-old mice and staining chromosome spreads of those mice by immunofluorescence using several antibodies. Similar to previous reports for Cdk2KO mice [38,50], spermatocytes from KI mice enter meiosis and progress through the first stages of prophase I (Figure 5 and Supplementary Figure S7). Sycp3 and Sycp1 are components of the synaptonemal complex and can be used for staging of cells during synapsis [51,52]. We stained spreads with antibodies against Sycp3 and found that both $Cdk2^{T160A}$ (Figure 5A) and WT (Supplementary Figure S7A) displayed comparable patterns from leptotene to pachytene. Staining with antibodies against Sycp1 revealed similar labeling from zygotene to pachytene in mutant and WT (Figure 5A and Supplementary Figure S7A). Similar to the chromosome spreads of control testes (Supplementary Figure S7A), spermatocytes from KI mutant T160A mice were able to reach the pachytene stage as indicated by the appearance of the localized phospho-H2AX signal, the strong condensation of homologous chromosomes visualized by Sycp3 staining, and a SUN1 signal at the ends of the synaptonemal complexes (Figure 5A and Supplementary Figure S7A) [38,50]. However, we were unable to observe any spermatocytes in a pachytene stage from testes extracted of $Cdk2^{D145N/D145N}$ mice (Figure 5B and Supplementary Figure S7B). In comparison with control mice 23 days after birth, the KI mutant T160A displays a decrease in the number of spermatocytes at diplotene stage, but an increase in zygotene-staged spermatocytes (Figure 5B). At this age, the first round of meiosis I has been completed as confirmed from our control mice and the appearance of all stages (Figure 5B and Supplementary Figure S7A,B). To exclude the possibility that there is only a delay but not a block in the progression of the meiosis I imposed by the $Cdk2^{T160A}$ mutant, we further analyzed the distribution of the different stages from testes isolated from 1-month-old mice. Although we observe a minimal increase in the number of spermatocytes in diplotene stage for the KI mutant T160A (<1% at P23 vs. ±5% at 1 month old), we were unable to observe any diakinesis, indicating that T160A testis are also blocked in development. To confirm that the phenotype observed for the T160A mutant is not due to mislocalization of the Cdk2, we stained the isolated spermatocytes for $Cdk2^{T160A}$ protein, which was localized like in the control $Cdk2^{+/+}$ cells at the telomeric end of the chromosomes as previously reported (Figure 5A and Supplementary Figure S7A) [38,50,53].

Taken together, these data indicate that enzymatically inactive Cdk2 does not adversely affect major aspects of host cell phenotype or function either *in vitro* or *in vivo*. This avoids engaging compensatory mechanisms that confound standard gene knockout approaches, but is nonetheless associated with defective meiosis and declining morphology and function of reproductive organs that lead to sterility.

Discussion

Here, we provide comprehensive data that indicate a critical requirement for kinase activity of Cdk2 in supporting meiotic cell division *in vivo*. By generating mice that expressed kinase-inactive forms of Cdk2, but retained normal expression of cell cycle regulatory proteins and complexes in these animals, we were able to demonstrate that loss of Cdk2 catalytic function alone is sufficient to disrupt normal gametogenesis. We tested many aspects of Cdk2 function, and in the majority of cases, both mice and cells that expressed the kinase-dead $Cdk2^{D145N}$ and $Cdk2^{T160A}$ point mutant alleles were indistinguishable from the well-documented phenotype of their Cdk2KO counterparts [5,9]. Our data indicate that the expression of enzymatically inactive Cdk2 at normal physiological levels does not act as a dominant-negative mutation and cannot rescue the sterility observed in Cdk2KO knockout animals. Since expression of the Cdk2 mutant alleles mimics the Cdk2KO situation, we conclude that the essential functions of Cdk2 are probably mediated by phosphorylating specific protein substrates. It would be interesting to determine the essential Cdk2 substrates in testis, which will be the focus of future studies. While kinase-independent functions have recently been reported for many cell cycle regulators, including cyclin E1 [10,11], cyclin D [12,13], and Cdk6 [14], we now provide compelling evidence that Cdk2 behaves like a classical kinase with few or no kinase-independent functions.

Our approach aimed to minimize perturbations to the endogenous Cdk2 locus while disrupting its kinase activity of the corresponding protein, thus ensuring that the regulation of the KI Cdk2 variant was not altered in comparison with WT. To this end, we made a single base-pair change G → A (433, D145N) or A → G (478, T160A) while leaving the remainder of the Cdk2 locus unchanged (except the single loxP recombination site left behind). Physiological expression levels of the KI Cdk2 protein were confirmed by both WB and qPCR; hence, this approach avoids the dominant-negative effects observed in transfected cell lines whereby $Cdk2^{D145N}$ is overexpressed and likely sequesters free cyclins away from WT Cdk proteins [24].

While both $Cdk2^{D145N}$ and $Cdk2^{T160A}$ were fully capable of binding to cyclins and Cdk inhibitory proteins, mutation of these different residues exerts distinct effects on Cdk2 functions. Asp145 is involved in coordinating Mg^{2+} ion to orientate ATP for catalysis by Cdk2 [20,21], whereas phosphorylation of Thr160 residue is essential for kinase activation [26]. Contrary to an earlier report, we were unable to detect basal kinase activity or autophosphorylation of $Cdk2^{T160A}$ in either tissue extracts or MEFs [54], suggesting that both Cdk2 mutant KIs are truly kinase-dead. Accordingly, the phenotypes observed for both $Cdk2^{D145N}$ and $Cdk2^{T160A}$ mutants were closely matched and comparable to Cdk2KO mice. The only distinction between these genotypes was the milder/delayed phenotype of declining ovary/testis morphology in $Cdk2^{T160A}$ animals. The underlying reasons for the milder phenotype of the T160A mutant, relative to the D145N mutant, are not clear, although this could be due to the reported ability of cyclin-like Speedy/RINGO proteins to activate $Cdk2^{T160A}$ with comparable efficacy to WT Cdk2 [55]. Indeed, Speedy proteins are expressed at much higher levels in ovary and testis than in other mouse tissues [55], and may therefore be capable of forming an active complex with $Cdk2^{T160A}$ and mitigating the effects of disrupted kinase function. Corroborating this hypothesis, it was recently shown

that Speedy A/RingoA knockout mice display a testis phenotype that is identical compared with Cdk2KO [56].

In summary, we have used both *in vitro* and *in vivo* systems to demonstrate that the kinase activity of Cdk2 is critically required for the normal physiological functions of this protein. Since the 'kinase-dead' Cdk2 protein is unable to support normal meiotic cell division *in vivo*, this enzyme must regulate biological processes exclusively by phosphorylating protein substrates. We would speculate that the same also holds true for Cdk1, although this has yet to be tested *in vivo*. As a critical regulator of meiotic cell division and potential target for the treatment of human cancers, these data both advance our current understanding of the processes that generate genetic variety via homologous recombination, and may lead to the development of novel therapies that modify DNA repair mechanisms in various malignancies.

Supplementary Material

Refer to Web version on PubMed Central for supplementary material.

Acknowledgements

We deeply appreciate the support and encouragement provided by all members of the Kaldis laboratory. We thank Eileen Southon and Susan Reid for help in generating the Cdk2^{T160A} and Cdk2^{D145N} mice. We also thank Zakiah Tablib, Chloe Sim, and Vithya Anantaraja for animal care; Daniel Chew for technical support; Brian Burke for antibodies against SUN1; and we acknowledge the technical expertise provided by the Advanced Molecular Pathology Laboratory at IMCB. The authors wish to thank Insight Editing London for their assistance in producing this manuscript.

Funding

P.K., S.C., M.K.D., J.H.S.L., X.B., V.M., C.K.R., B.J., J.N., and F.G. acknowledge the support by the Biomedical Research Council of A*STAR (Agency for Science, Technology and Research), Singapore. D.A. and K.L. were supported by grants (to K.L.) from the Jane and Dan Olssons Foundation, the LUA/ALF-medel Västra Götalandsregionen, AFA Insurance, the Swedish Research Council, and the Swedish Cancer Foundation. V.C. and L.T. were supported by the Intramural Research Program of the NIH, National Cancer Institute, Center for Cancer Research.

Abbreviations

A/A	homozygous for alanine mutation
AFU	arbitrary fluorescence unit
amino acid A	alanine
amino acid D	aspartic acid
amino acid N	asparagine
amino acid T	threonine
Asp	aspartic acid
Cdks	cyclin-dependent kinases
D145N	aspartic acid to asparagine mutation

ES	cell embryonic stem cell
FACS	fluorescence-activated cell sorting
H1	histone H1
HBSS	Hanks' balanced salt solution
IP	immunoprecipitation
KI	knockin
KO	knockout
N/N	homozygous for asparagine mutation
PCR	polymerase chain reaction
PI	propidium iodide
qPCR	quantitative polymerase chain reaction
RasG12V	Ras glycine 12 to valine mutation
shRNA	small hairpin ribonucleic acid
T160A	threonine to alanine mutation
Thr	threonine
WB	Western blot
WT	wild type

References

1. Morgan DO. (2007) The Cell Cycle: Principles of Control (Lawrence E, ed.), New Science Press Ltd, London
2. Aleem E, Berthet C and Kaldis P. (2004) Cdk2 as a master of S phase entry: fact or fake? Cell Cycle 3, 34–36 doi:10.4161/cc.3.1.632
3. Aleem E and Kaldis P. (2006) Mouse models of cell cycle regulators: new paradigms. Results Probl. Cell Differ 42, 271–328 doi:10.1007/400_023 [PubMed: 16903215]
4. Aleem E, Kiyokawa H and Kaldis P. (2005) Cdc2-cyclin E complexes regulate the G1/S phase transition. Nat. Cell Biol 7, 831–836 doi:10.1038/ncb1284 [PubMed: 16007079]
5. Berthet C, Aleem E, Coppola V, Tessarollo L and Kaldis P. (2003) Cdk2 knockout mice are viable. Curr. Biol 13, 1775–1785 doi:10.1016/j.cub.2003.09.024 [PubMed: 14561402]
6. Berthet C and Kaldis P. (2006) Cdk2 and Cdk4 cooperatively control the expression of Cdc2. Cell Div 1, 10 doi:10.1186/1747-1028-1-10 [PubMed: 16759374]
7. Berthet C and Kaldis P. (2007) Cell-specific responses to loss of cyclin-dependent kinases. Oncogene 26, 4469–4477 doi:10.1038/sj.onc.1210243 [PubMed: 17297466]
8. Berthet C, Klarmann KD, Hilton MB, Suh HC, Keller JR, Kiyokawa H. et al. (2006) Combined loss of Cdk2 and Cdk4 results in embryonic lethality and Rb hypophosphorylation. Dev. Cell 10, 563–573 doi:10.1016/j.devcel.2006.03.004 [PubMed: 16678773]

9. Ortega S, Prieto I, Odajima J, Martín A, Dubus P, Sotillo R. et al. (2003) Cyclin-dependent kinase 2 is essential for meiosis but not for mitotic cell division in mice. Nat. Genet 35, 25–31 doi:10.1038/ng1232 [PubMed: 12923533]
10. Geng Y, Lee Y-M, Welcker M, Swanger J, Zagozdzon A, Winer JD. et al. (2007) Kinase-independent function of cyclin E. Mol. Cell 25, 127–139 doi:10.1016/j.molcel.2006.11.029 [PubMed: 17218276]
11. Odajima J, Wills ZP, Ndassa YM, Terunuma M, Kretschmannova K, Deeb TZ. et al. (2011) Cyclin E constrains Cdk5 activity to regulate synaptic plasticity and memory formation. Dev. Cell 21, 655–668 doi:10.1016/j.devcel.2011.08.009 [PubMed: 21944720]
12. Bienvenu F, Jirawatnotai S, Elias JE, Meyer CA, Mizeracka K, Marson A. et al. (2010) Transcriptional role of cyclin D1 in development revealed by a genetic-proteomic screen. Nature 463, 374–378 doi:10.1038/nature08684 [PubMed: 20090754]
13. Jirawatnotai S, Hu Y, Michowski W, Elias JE, Becks L, Bienvenu F. et al. (2011) A function for cyclin D1 in DNA repair uncovered by protein interactome analyses in human cancers. Nature 474, 230–234 doi:10.1038/nature10155 [PubMed: 21654808]
14. Kollmann K, Heller G, Schneckenleithner C, Warsch W, Scheicher R, Ott RG. et al. (2013) A kinase-independent function of CDK6 links the cell cycle to tumor angiogenesis. Cancer Cell 24, 167–181 doi:10.1016/j.ccr.2013.07.012 [PubMed: 23948297]
15. Connell-Crowley L, Solomon MJ, Wei N and Harper JW. (1993) Phosphorylation independent activation of human cyclin-dependent kinase 2 by cyclin A in vitro. Mol. Biol. Cell 4, 79–92 doi:10.1091/mbc.4.1.79 [PubMed: 8443411]
16. Gu Y, Rosenblatt J and Morgan DO. (1992) Cell cycle regulation of CDK2 activity by phosphorylation of Thr160 and Tyr15. EMBO J 11, 3995–4005 PMID: 1396589 [PubMed: 1396589]
17. Kaldis P, Cheng A and Solomon MJ. (2000) The effects of changing the site of activating phosphorylation in CDK2 from threonine to serine. J. Biol. Chem 275, 32578–32584 doi:10.1074/jbc.M003212200 [PubMed: 10931829]
18. Kaldis P, Russo AA, Chou HS, Pavletich NP and Solomon MJ. (1998) Human and yeast cdk-activating kinases (CAKs) display distinct substrate specificities. Mol. Biol. Cell 9, 2545–2560 doi:10.1091/mbc.9.9.2545 [PubMed: 9725911]
19. Solomon MJ, Lee T and Kirschner MW. (1992) Role of phosphorylation in p34cdc2 activation: identification of an activating kinase. Mol. Biol. Cell 3, 13–27 doi:10.1091/mbc.3.1.13 [PubMed: 1532335]
20. De Bondt HL, Rosenblatt J, Jancarik J, Jones HD, Morgan DO and Kim S-H. (1993) Crystal structure of cyclin-dependent kinase 2. Nature 363, 595–602 doi:10.1038/363595a0 [PubMed: 8510751]
21. Jeffrey PD, Russo AA, Polyak K, Gibbs E, Hurwitz J, Massagué J. et al. (1995) Mechanism of cdk activation revealed by the structure of a cyclin A-CDK2 complex. Nature 376, 313–320 doi:10.1038/376313a0 [PubMed: 7630397]
22. Hu B, Mitra J, van den Heuvel S and Enders GH. (2001) S and G2 phase roles for cdk2 revealed by inducible expression of a dominant-negative mutant in human cells. Mol. Cell. Biol 21, 2755–2766 doi:10.1128/MCB.21.8.2755-2766.2001 [PubMed: 11283255]
23. Mitra J and Enders GH. (2004) Cyclin A/Cdk2 complexes regulate activation of Cdk1 and Cdc25 phosphatases in human cells. Oncogene 23, 3361–3367 doi:10.1038/sj.onc.1207446 [PubMed: 14767478]
24. van den Heuvel S and Harlow E. (1993) Distinct roles for cyclin-dependent kinases in cell cycle control. Science 262, 2050–2054 doi:10.1126/science.8266103 [PubMed: 8266103]
25. Fisher RP and Morgan DO. (1994) A novel cyclin associates with M015/CDK7 to form the CDK-activating kinase. Cell 78, 713–724 doi:10.1016/0092-8674(94)90535-5 [PubMed: 8069918]
26. Kaldis P. (1999) The cdk-activating kinase (CAK): from yeast to mammals. Cell. Mol. Life Sci 55, 284–296 doi:10.1007/s000180050290 [PubMed: 10188587]
27. Kaldis P. (2002) The CDK-activating Kinase (CAK) R. G. Landes Com, Austin, TX
28. Kaldis P, Sutton A and Solomon MJ. (1996) The Cdk-activating kinase (CAK) from budding yeast. Cell 86, 553–564 doi:10.1016/S0092-8674(00)80129-4 [PubMed: 8752210]

29. Shuttleworth J, Godfrey R and Colman A. (1990) p40^{MO15}, a *cdc2*-related protein kinase involved in negative regulation of meiotic maturation of Xenopus oocytes. EMBO J 9, 3233–3240 PMID: 2209545 [PubMed: 2209545]
30. Solomon MJ, Harper JW and Shuttleworth J. (1993) CAK, the p34^{cdc2} activating kinase, contains a protein identical or closely related to p40MO15. EMBO J 12, 3133–3142 PMID: 8344252 [PubMed: 8344252]
31. Lee E-C, Yu D, Martinez de Velasco J, Tessarollo L, Swing DA, Court DL. et al. (2001) A highly efficient Escherichia coli-based chromosome engineering system adapted for recombinogenic targeting and subcloning of BAC DNA. Genomics 73, 56–65 doi:10.1006/geno.2000.6451 [PubMed: 11352566]
32. Rodríguez CI, Buchholz F, Galloway J, Sequerra R, Kasper J, Ayala R. et al. (2000) High-efficiency deleter mice show that FLPe is an alternative to Cre-loxP. Nat. Genet 25, 139–140 doi:10.1038/75973 [PubMed: 10835623]
33. Truett GE, Heeger P, Mynatt RL, Truett AA, Walker JA and Warman ML. (2000) Preparation of PCR-quality mouse genomic DNA with hot sodium hydroxide and Tris (HotSHOT). Biotechniques 29, 52, 54 PMID: 10907076 [PubMed: 10907076]
34. Diril MK, Ratnacaram CK, Padmakumar VC, Du T, Wasser M, Coppola V. et al. (2012) Cyclin-dependent kinase 1 (Cdk1) is essential for cell division and suppression of DNA re-replication but not for liver regeneration. Proc. Natl Acad. Sci. USA 109, 3826–3831 doi:10.1073/pnas.1115201109 [PubMed: 22355113]
35. Luche H, Ardouin L, Teo P, See P, Henri S, Merad M. et al. (2011) The earliest intrathymic precursors of CD8α+ thymic dendritic cells correspond to myeloid-type double-negative 1c cells. Eur. J. Immunol 41, 2165–2175 doi:10.1002/eji.201141728 [PubMed: 21630253]
36. Schlitzer A, McGovern N, Teo P, Zelante T, Atarashi K, Low D. et al. (2013) IRF4 transcription factor-dependent CD11b^{+} dendritic cells in human and mouse control mucosal IL-17 cytokine responses. Immunity 38, 970–983 doi:10.1016/j.immuni.2013.04.011 [PubMed: 23706669]
37. Peters HFM, Plug AW, van Vugt MJ and de Boer P. (1997) A drying-down technique for the spreading of mammalian meiocytes from the male and female germline. Chromosome Res. 5, 66–68 doi:10.1023/A:1018445520117 [PubMed: 9088645]
38. Viera A, Rufas JS, Martinez I, Barbero JL, Ortega S and Suja JA. (2009) CDK2 is required for proper homologous pairing, recombination and sex-body formation during male mouse meiosis. J. Cell Sci 122, 2149–2159 doi:10.1242/jcs.046706 [PubMed: 19494131]
39. Adon AM, Zeng X, Harrison MK, Sannem S, Kiyokawa H, Kaldis P. et al. (2010) Cdk2 and Cdk4 regulate the centrosome cycle and are critical mediators of centrosome amplification in p53-null cells. Mol. Cell. Biol 30, 694–710 doi:10.1128/MCB.00253-09 [PubMed: 19933848]
40. Campaner S, Doni M, Hydbring P, Verrecchia A, Bianchi L, Sardella D. et al. (2010) Cdk2 suppresses cellular senescence induced by the c-myc oncogene. Nat. Cell Biol 12, 54–59 doi:10.1038/ncb2004 [PubMed: 20010815]
41. Duensing A, Liu Y, Tseng M, Malumbres M, Barbacid M and Duensing S. (2006) Cyclin-dependent kinase 2 is dispensable for normal centrosome duplication but required for oncogene-induced centrosome overduplication. Oncogene 25, 2943–2949 doi:10.1038/sj.onc.1209310 [PubMed: 16331279]
42. Kotoshiba S, Gopinathan L, Pfeiffenberger E, Rahim A, Vardy LA, Nakayama K. et al. (2014) p27 is regulated independently of Skp2 in the absence of Cdk2. Biochim. Biophys. Acta 1843, 436–445 doi:10.1016/j.bbamcr.2013.11.005 [PubMed: 24269842]
43. Li W, Kotoshiba S, Berthet C, Hilton MB and Kaldis P. (2009) Rb/Cdk2/Cdk4 triple mutant mice elicit an alternative mechanism for regulation of the G1/S transition. Proc. Natl Acad. Sci. USA 106, 486–491 doi:10.1073/pnas.0804177106 [PubMed: 19129496]
44. Padmakumar VC, Aleem E, Berthet C, Hilton MB and Kaldis P. (2009) Cdk2 and Cdk4 activities are dispensable for tumorigenesis caused by the loss of p53. Mol. Cell. Biol 29, 2582–2593 doi:10.1128/MCB.00952-08 [PubMed: 19307310]
45. Bettencourt-Dias M and Glover DM. (2007) Centrosome biogenesis and function: centrosomics brings new understanding. Nat. Rev. Mol. Cell Biol 8, 451–463 doi:10.1038/nrm2180 [PubMed: 17505520]

46. Meraldi P, Lukas J, Fry AM, Bartek J and Nigg EA. (1999) Centrosome duplication in mammalian somatic cells requires E2F and Cdk2-cyclin A. Nat. Cell Biol 1, 88–93 doi:10.1038/10054 [PubMed: 10559879]
47. Fukasawa K, Choi T, Kuriyama R, Rulong S and Vande Woude GF. (1996) Abnormal centrosome amplification in the absence of p53. Science 271, 1744–1747 doi:10.1126/science.271.5256.1744 [PubMed: 8596939]
48. Liu X and Erikson RL. (2002) Activation of Cdc2/cyclin B and inhibition of centrosome amplification in cells depleted of Plk1 by siRNA. Proc. Natl Acad. Sci. USA 99, 8672–8676 doi:10.1073/pnas.132269599 [PubMed: 12077309]
49. Adhikari D, Zheng W, Shen Y, Gorre N, Ning Y, Halet G. et al. (2012) Cdk1, but not Cdk2, is the sole Cdk that is essential and sufficient to drive resumption of meiosis in mouse oocytes. Hum. Mol. Genet 21, 2476–2484 doi:10.1093/hmg/dds061 [PubMed: 22367880]
50. Viera A, Alsheimer M, Gomez R, Berenguer I, Ortega S, Symonds CE. et al. (2015) Cdk2 regulates nuclear envelope protein dynamics and telomere attachment in mouse meiotic prophase. J. Cell Sci 128, 88–99 doi:10.1242/jcs.154922 [PubMed: 25380821]
51. Hamer G, Gell K, Kouznetsova A, Novak I, Benavente R and Hoog C. (2006) Characterization of a novel meiosis-specific protein within the central element of the synaptonemal complex. J. Cell Sci 119, 4025–4032 doi:10.1242/jcs.03182 [PubMed: 16968740]
52. Lin F-J, Shen L, Jang C-W, Falnes PO and Zhang Y. (2013) Ikbkap/Elp1 deficiency causes male infertility by disrupting meiotic progression. PLoS Genet 9, e1003516 doi:10.1371/journal.pgen.1003516 [PubMed: 23717213]
53. Ashley T, Walpita D and de Rooij DG. (2001) Localization of two mammalian cyclin dependent kinases during mammalian meiosis. J. Cell Sci 114 (Pt 4), 685–693 PMID: 11171374 [PubMed: 11171374]
54. Brown NR, Noble MEM, Lawrie AM, Morris MC, Tunnah P, Divita G. et al. (1999) Effects of phosphorylation of threonine 160 on cyclin-dependent kinase 2 structure and activity. J. Biol. Chem 274, 8746–8756 doi:10.1074/jbc.274.13.8746 [PubMed: 10085115]
55. Chauhan S, Zheng X, Tan Y-Y, Tay B-H, Lim S, Venkatesh B. et al. (2012) Evolution of the Cdk-activator Speedy/RINGO in vertebrates. Cell Mol. Life Sci 69, 3835–3850 doi:10.1007/s00018-012-1050-1 [PubMed: 22763696]
56. Mikolcevic P, Isoda M, Shibuya H, del Barco Barrantes I, Igea A, Suja JA. et al. (2016) Essential role of the Cdk2 activator RingoA in meiotic telomere tethering to the nuclear envelope. Nat. Commun 7, 11084 doi:10.1038/ncomms11084 [PubMed: 27025256]

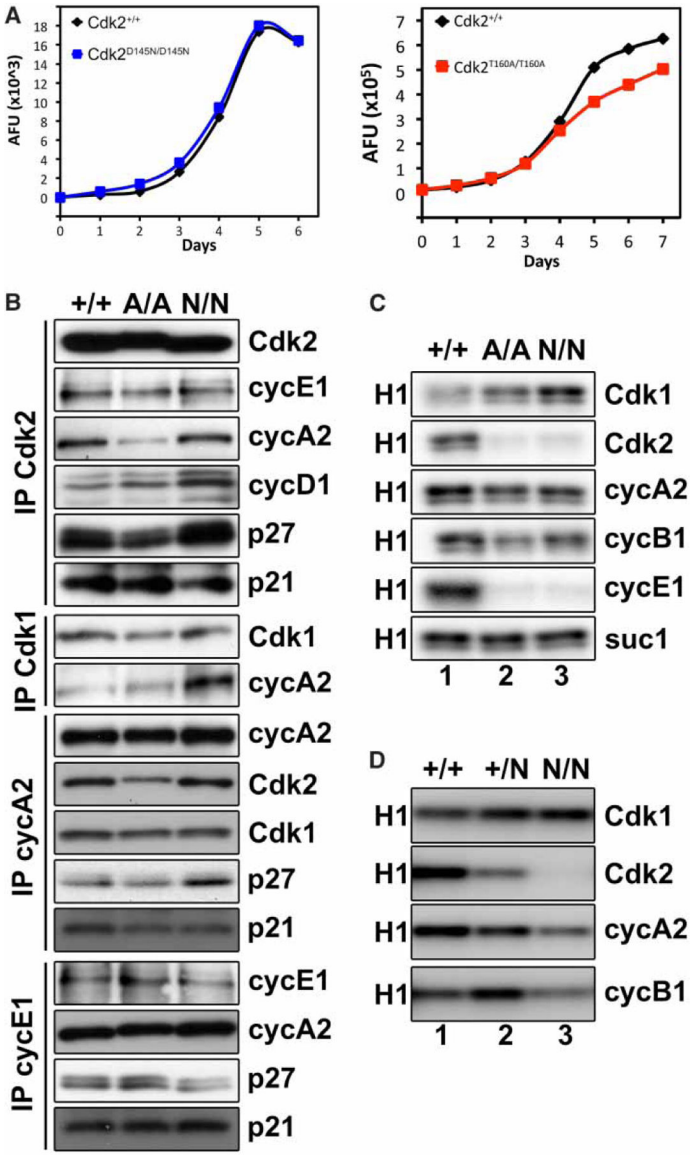

Figure 1. Cdk2^{T160A} and Cdk2^{D145N} MEFs exhibit normal mitotic proliferation potential.

(A) Proliferation assays using Alamar Blue staining after serum starvation/release are shown for wild-type MEFs (black), Cdk2$^{T160A/T160A}$ MEFs (red), and Cdk2$^{D145N/D145N}$ MEFs (blue). Representative pictures from more than three experiments from independent embryos are shown. **(B)** Composition of complexes was determined after IP using antibodies against Cdk2, Cdk1, cyclin A2, and cyclin E1 followed by Western blotting with the indicated antibodies. (**C** and **D**) Kinase activity was determined *in vitro* using radiolabeled ATP and histone H1 as substrates. Cdk/cyclin complexes were immunoprecipitated using the indicated antibodies and kinase assays were performed on beads as described in Materials and Methods (+/+ indicates wild type, A/A Cdk2$^{T160A/T160A}$, +/N Cdk2$^{+/D145N}$, and N/N Cdk2$^{D145N/D145N}$).

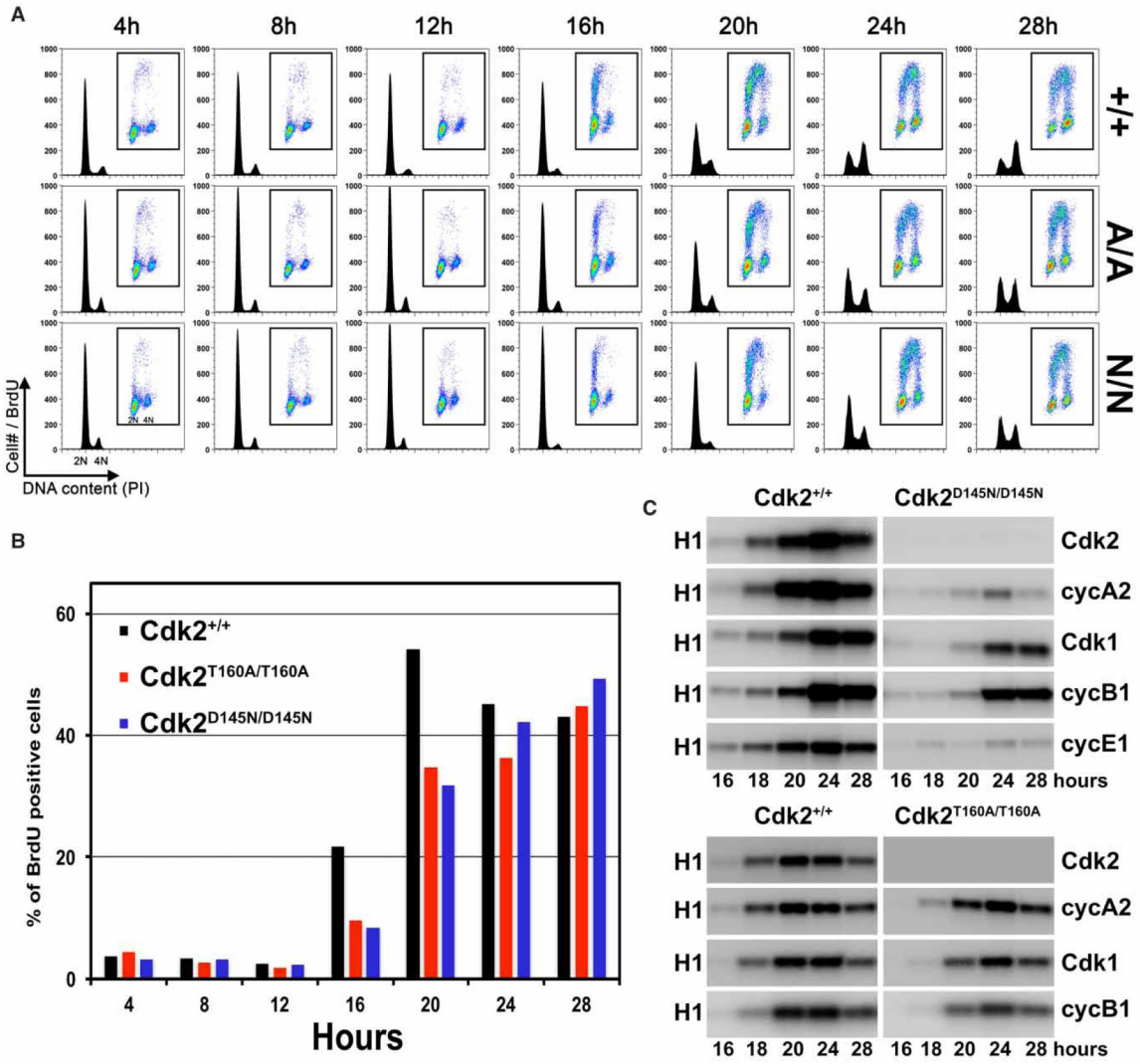

Figure 2. Cell cycle progression in Cdk2^{D145N} and Cdk2^{T160A} KI MEFs.

(A) Primary wild-type MEFs (black), Cdk2$^{T160A/T160A}$ MEFs (red), and Cdk2$^{D145N/D145N}$ MEFs (blue) were grown to confluency, serum-starved for 72 h, and then released synchronously into cell cycle by re-plating in medium containing 10% serum. Cells were collected at the indicated time points, pulse-labeled for 1 h with BrdU and propidium iodine, and then analyzed by FACS. Data were processed using FlowJo software. **(B)** Graph of FACS data from **(A)**. The data shown are representative from more than three replicates with MEFs from different embryos. **(C)** At the indicated time points after re-plating in 10% serum medium, cells were harvested and protein extracts prepared. After IP with the indicated antibodies, Cdk/cyclin complexes were subjected to *in vitro* kinase assays using radiolabeled ATP and histone H1 as substrates as described in Materials and Methods. Comparison of MEFs from wild-type and Cdk2$^{D145N/D145N}$ (upper panel) or Cdk2$^{T160A/T160A}$ (lower panel) animals is shown. Neither of the Cdk2 mutants displayed any measurable kinase activity.

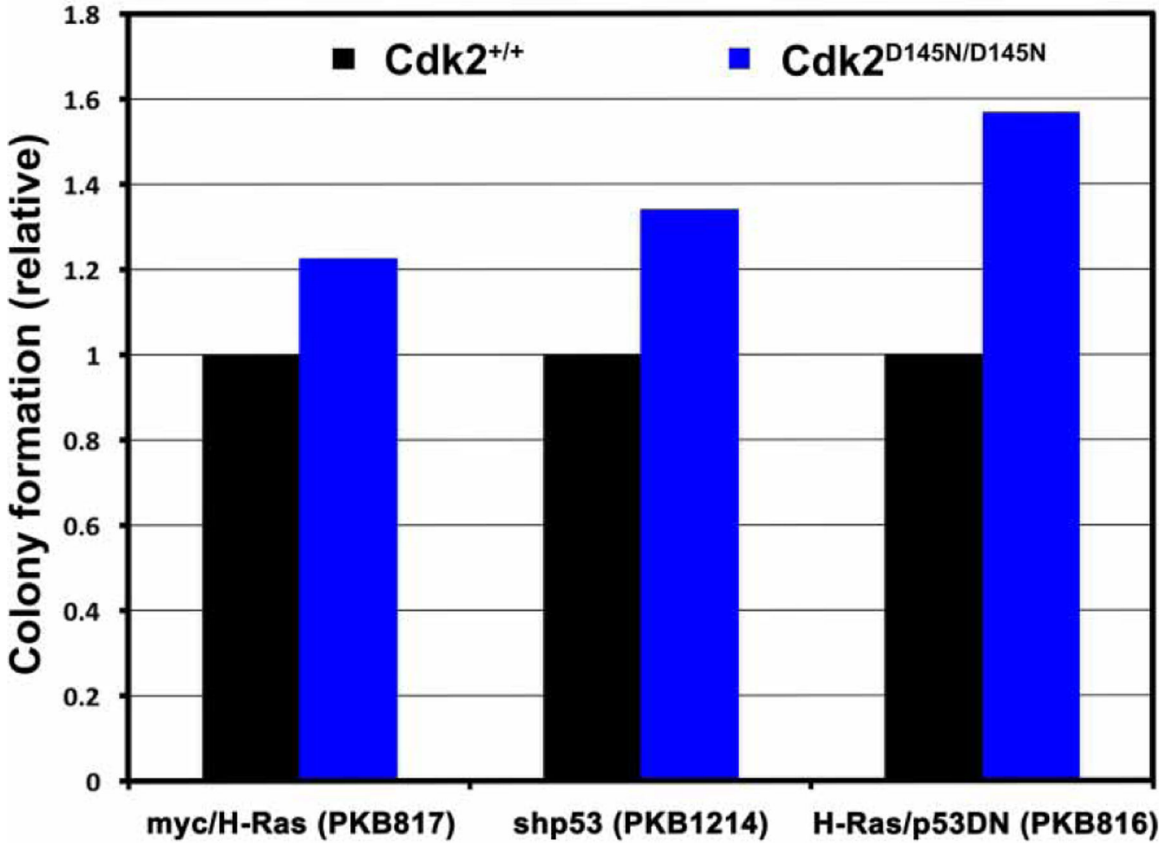

Figure 3. Efficient transformation of Cdk2^{D145N} MEFs.

Wild-type MEFs (black) and Cdk2^{D145N} MEFs (blue) were infected with retroviruses encoding for c-myc and activated H-Ras (PKB817), shRNA to silence p53 (PKB1214), or activated H-Ras and p53^{DN} (dominant negative; PKB816). A total of 2000 cells were seeded per 10 cm dish and the resultant colonies were counted 2 weeks later. The number of colonies varied for each vector and was therefore normalized to the number of colonies from wild-type MEFs.

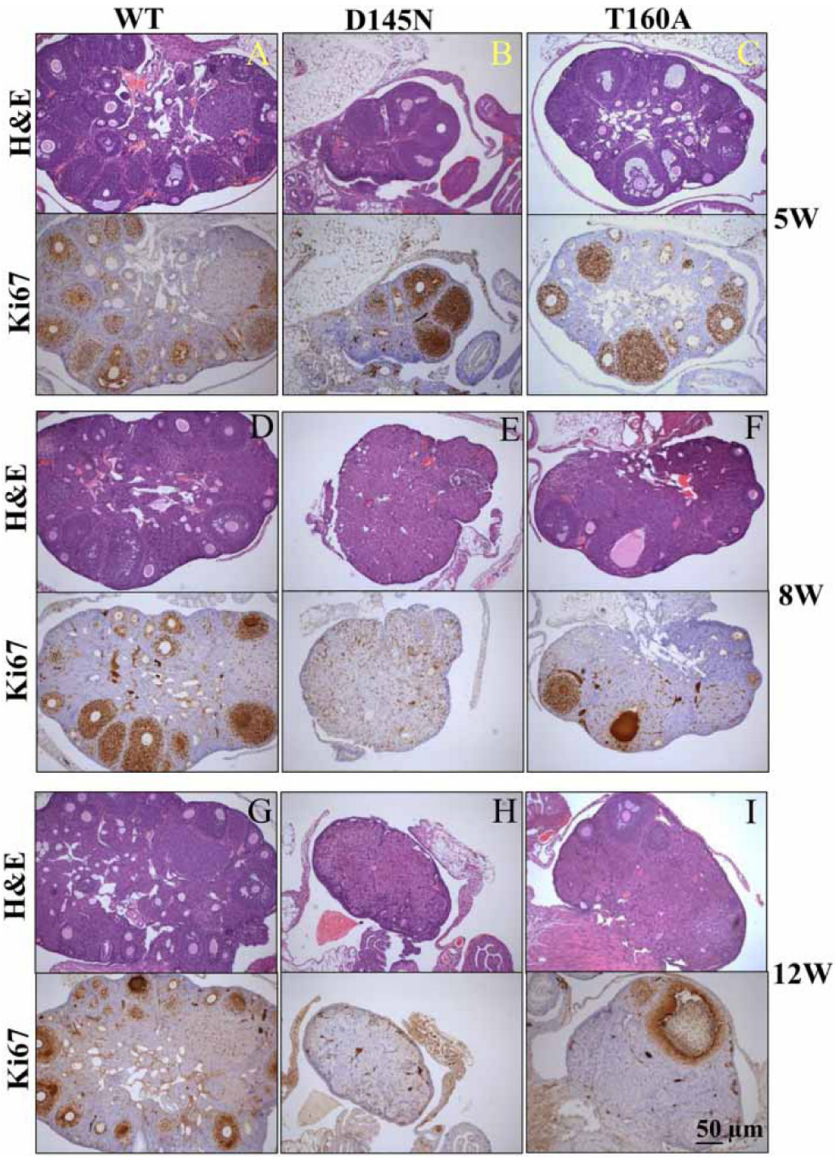

Figure 4. Progressive decline in ovarian morphology in Cdk2^{T160A} and Cdk2^{D145N} mice.

(A–I) Ovaries were collected from WT, D145N, and T160A mice at 5, 8, or 12 weeks of age, then embedded in paraffin and cut into sections. Near-identical sections from the same organ were either stained with H&E or immunostained with antibodies against Ki67. At 5 weeks of age, D145N ovaries appeared much smaller and contained fewer follicles than those obtained from WT mice (**A** and **B**). In T160A mice, ovary sizes and follicle numbers at 5 weeks were intermediate between those of WT and D145N animal (**C**). Ovaries from 8-week-old WT mice contained multiple different types of follicles (**D**), whereas few follicles remained in ovaries from T160A mice of the same age (**F**), and follicles were entirely absent from the ovaries of D145N mice at this time point (**E**). By 12 weeks of age, D145N ovaries completely lacked follicles or cycling cells and appeared wasted (**H**), whereas T160A ovaries were almost devoid of follicles and cycling cells (**I**). WT control ovaries contained a range of healthy follicles at various developmental stages (**G**).

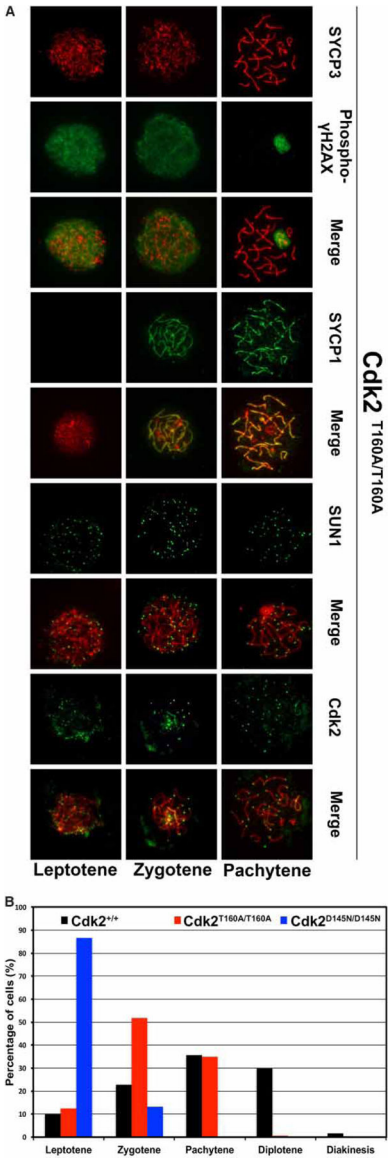

Figure 5. Spermatocytes from Cdk2^{T160A} and Cdk2^{D145N} KI mice arrest during prophase I.

(A) Immunostaining with antibodies against the indicated markers on chromosome spreads from testes extracted of Cdk2$^{T160/T160A}$ mice at postnatal day 23. The merged images correspond to the staining of Sycp3 in red and the staining of indicated proteins above it. **(B)** Quantification of the percentage of spermatocytes identified in each stage of prophase I based on Sycp3 staining. Spermatocytes were extracted from testes of Cdk2$^{+/+}$ (total cell count $n = 317$), Cdk2$^{T160A/T160A}$ ($n = 338$), and Cdk2$^{D145N/D145N}$ ($n = 150$) mice at postnatal day 23.

Table 1

Oligonucleotide primers used in this study

Primer name	Primer sequence (5′ → 3′)
5′ Probe forward, PKO116	CTAGCAGAGTGCGGACCTGAGC
5′ Probe reverse, PKO117	GCTACATTGCTTAAGGTCCAGGCC
3′ Probe forward, PKO1336	GGAGCCGAGCCTCTAGTTG
3′ Probe reverse, PKO1337	TCACCACACCCAAGCACTAA
PKO956, D145N mutagenesis	CTCTTGCTAGTCCAAAGT**T**TGCCAGCTTGA
PKO957, D145N mutagenesis	TCAAGCTGGCA**A**ACTTTGGACTAGCAAGAG
PKO959, T160A mutagenesis	TGTCCGAACTTAC**G**CTCATGAGGTAAGTC
PKO960, T160A mutagenesis	GACTTACCTCATGAG**C**GTAAGTTCGGACA
Genotyping Pr1, PKO2142	CGTGGCTCTAACTTTTAC
Genotyping Pr2, PKO2143	GGAAACTTAACTCAGGTC

Table 2

Quantitative PCR primers used in this study

Primer name	Primer sequence (5′ → 3′)
Cdk1; PKR196— Fwd	AGCGAGGAAGAAGGAGTGCC
Cdk1; PKR196— Rev	CATGAGCACATCCTGCAGGC
Cyclin E1; PKR277— Fwd	ACAGCTTCGGGTCTGAGTTC
Cyclin E1; PKR277— Rev	CGGAGCCACCTTCTTCTTTC
Cyclin A2; PKR270— Fwd	CAACCCCGAAAAACTGGCGC
Cyclin A2; PKR270— Rev	AAGAGGAGCAACCCGTCGAG
Cdk2; PKR047— Fwd	GGGTCCATCAAGCTGGCAGA
Cdk2; PKR047— Rev	CCACAGGGTCACCACCTCAT

Table 3

Results for heterozygote intercrosses of $Cdk2^{D145N}$ or $Cdk2^{T160A}$ mice

Genotype	+/+	+/D145N	D145N/D145N	Total
Number of mice	169	296	75	540
Percentage	31.3	54.8	13.9	100
Genotype	+/+	+/T160A	T160A/T160A	Total
Number of mice	169	295	96	560
Percentage	30.2	52.7	17.1	100